Computers and Electronics in Agriculture 229 (2025) 109709

Contents lists available at ScienceDirect

Computers and Electronics in Agriculture

journal homepage: www.elsevier.com/locate/compag

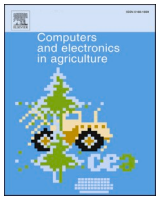

Original papers

Non-destructive assessment of the internal defects of FRED® pear by a low radio-frequency capacitive technique

Eleonora Iaccheri [a,b,*], Annachiara Berardinelli [c,d], Gianni Ceredi [e], Luigi Ragni [a,b]

[a] Interdepartmental Centre for Agri-Food Industrial Research, Alma Mater Studiorum, University of Bologna, Cesena, Italy
[b] Department of Agricultural and Food Science, Alma Mater Studiorum, University of Bologna, Cesena, Italy
[c] Center of Agriculture Food Environment C3A, University of Trento, Via Edmund Mach 1, 38098 San Michele all'Adige, Trento, Italy
[d] Department of Industrial Engineering, University of Trento, Via Sommarive, 9, 38123 Povo, Italy
[e] APOFRUIT ITALIA Soc. Coop. Ar.L., Viale della Cooperazione, 400, Cesena, Italy

ARTICLE INFO

Keywords:
Fruit quality
Internal defect
Non-destructive assessment
Pear
Radiofrequency

ABSTRACT

Postharvest pear fruit internal browning damages were assessed non-destructively using a capacitive instrumental chain in the super low (SLF) – low (LF) radiofrequency region combined with Image analysis. A rapid, inexpensive, and non-destructive instrumental chain was set up: an LCR meter interfaced with a PC receives and transmits signals through a parallel plate capacitor in the frequency range from 100 Hz to 10 kHz. The capacitance data were used to classify the FRED® pear fruit into two classes, "with defects" and "healthy", using the unsupervised fuzzy C-means clustering analysis. The main results show good classification rates: 91 % of the samples are correctly classified as damaged. Further samples should be implemented to understand how the model performs with samples from different ripening stages. Despite this, the technique appears promising for non-destructive internal quality assessment in pear fruit.

1. Introduction

After harvesting, pears *(Pyrus communis L.)* fruits are stored under a controlled atmosphere (CA) to delay senescence phenomena and increase shelf life (Evans, 2020). The well-known postharvest storage aims at reducing the fruit respiration rate and metabolic processes by controlling and managing CO_2 and O_2 partial pressures, in addition to a temperature reduction (Teixeira and Ferreira, 2003). Due to the susceptibility to CO_2 levels, during long-term storage under a controlled atmosphere, internal flesh browning disorders with or without the development of cavities can occur (Streif et al., 2001). The process could be due to the increase in the internal gas concentrations above the toxic level for the product and first disorders can be observed starting from the beginning of storage and becoming more severe during this last (Franck et al., 2007). Browning disorder symptoms appeared to be related to the oxidation of phenolic compounds occurring after the breakdown of the cellular integrity associated with the accumulation of fermentative metabolites (Lwin et al., 2023). Factors such as cultivar, orchard practice, and harvest maturity can also have a role in the disorder development (Franck et al., 2007). Since the symptoms are internal and affect the inner part of the cortical parenchyma, the occurrence and the severity of the disorder cannot be assessed through an external quality assessment. In addition, the damage is extremely severe leading to important losses.

To identify optimal postharvest storage conditions and sort fruits according also to internal quality, some non-destructive assessment techniques have been explored, in combination with machine learning tools, to identify and quantify internal fruit disorders during postharvest storage, mainly at laboratory scale. These techniques undoubtedly include Magnetic resonance imaging (MRI), X-ray computer tomography (CT), spectroscopy as transmission Vis/NIR and time-resolved reflectance), and acoustic vibration signals (Lammertyn et al., 2003; Mei and Li, 2023; Nugraha et al., 2019; Zhao et al., 2021).

In MRI, changes in the chemical composition and structure influence the relaxation times of the protons in water and, consequently, the generated two-dimensional and three-dimensional MR images, under static magnetic fields and radio frequencies (Clark et al., 1997). The technique was successfully explored to detect internal browning in 'Blanquilla' pears (Hernández-Sánchez et al., 2007) and the spatial distribution of core breakdown in "Conference" pears (Lammertyn et al., 2003) but is characterized by a low image acquisition speed and high equipment costs (Colnago et al., 2014). Similarly, X-ray CT images,

* Corresponding author.
E-mail address: eleonora.iaccheri4@unibo.it (E. Iaccheri).

https://doi.org/10.1016/j.compag.2024.109709
Received 7 October 2024; Received in revised form 11 November 2024; Accepted 25 November 2024
Available online 2 December 2024

providing three-dimensional assessments of tissue density in combination with deep learning models, are considered still challenging complex, and expensive tools compared with other non-destructive technologies (Carmignato et al., 2017), even if interesting research works refer to the identification of internal browning and cavities in pear fruit (Tempelaere et al., 2023; Van De Looverbosch et al., 2022; Van De Looverbosch et al., 2020).

In the field of nondestructive evaluation of agricultural products, spectroscopic techniques can be considered the most diffused solutions, especially for their suitability for online applications and a few millimeters of superficial exploration. Some examples focused on internal inspection include Vis/NIR tools in transmission mode in the 651–1282 nm region for the detection of brown core in "Yali" pears (Han et al., 2006) and in the 550–1100 nm region for the moldy core classification in "Ya" pears (Zhang et al., 2022), and time-resolved reflectance spectroscopy at 690 and 720 nm for the identification of brown heart in "Conference" fruits based on photon adsorption and scattering events (Zerbini et al., 2002).

Pear internal disorders appeared, in addition, to affect the response of the fruit to vibroacoustic signals as testified by the recent work conducted by using contact piezoelectric transducers and different types of domain features (time and frequency) for the discrimination between healthy and browning pears (Zhang et al., 2024).

A promising reliable and powerful alternative applicative solution could be represented by techniques based on fruit dielectric properties. The numerous published works focused on fruit non-destructive maturity assessment, clearly evidence a relationship between the fruit's attributes (internal structure, moisture content, and chemical composition) and the dielectric permittivity at different ranges of frequencies measured with different probes (Khaled et al., 2015; Sipahioglu and Barringer, 2003).

Examples refer to a coaxial probe in the regions of 200–3000 MHz (Cao et al., 2023) and 20 MHz/MHz^{-4500}(−|-) MHz (Guo et al., 2015), a 2–20 GHz waveguide where the fruit is placed inside between two vertical antennas (Ragni et al., 2012), a contactless 947–1900 MHz waveguide device (Berardinelli et al., 2021), and to a rectangular parallel plate capacitor in the 10 kHz–10 MHz frequency range (Soltani et al., 2011a). Depending on the frequencies and type of instrumental chain, the techniques based on the exploration of the dielectric behavior have been proven to be rapid, low cost, suitable for online measurements, and with a good product penetration depth. These properties are undoubtedly interesting for the assessment of fruit internal chemical and physical changes due to diseases occurring during postharvest storage, especially in combination with simple machine learning tools.

AIM: The present research aims to explore the potentiality of a radiofrequency device for the non-destructive assessment of internal damages of a new variety of pear fruit during postharvest storage. Internal flesh browning disorders were assessed in the frequency range from 100 Hz to 10 kHz by using a self-assembled instrumental chain characterized by a stainless-steel parallel plate capacitor and an LCR meter interfaced with a PC. The acquired capacitance values in the explored frequency range were used as input data for Fuzzy-C means clustering analysis intending to discriminate between internally defective and healthy pear fruits. t-distributed Stochastic Neighbor Embedding (t-SNE) algorithm was used to manage high-dimensional data and project the observations into a 2D-dimensional space.

2. Material and methods

2.1. Experimental design

Observation and results of this article were obtained from pear fruit of FRED® variety following the experimental design shown in Fig. 1.

The harvest ended at a defined ripeness stage characterized by dimensional and quality indexes shown in the figure at point 1. Postharvest, after the sorting procedure and methodically packing fruit into crates was conducted in a refrigerated chamber with controlled storage conditions (point 2). After about four months of storage, samples were transported to the laboratory for data collection, numbered in figure as point 3. Firstly, non-destructive measurements were conducted, particularly the capacitance acquisition. Images of pears were acquired soon after the capacitive measurements, by cutting fruits. Following the experimental plan diagram, data analysis was the final step (point 4). The pear fruit images were used to calculate the number of pixels of the defect area and the number of pixels of the whole pear. The ratio between these two values was used as a defect percentage. A threshold of 2 % was defined for the healthy class because no defect, or only little browning is visible. Subsequently, capacitive measurements were used to classify samples by means of the Fuzzy-C means algorithm.

2.2. Plant materials and post-harvest handling

Two batches with 59 fruits of Italian FRED ® pears (*Pyrus communis L.)* were harvested from a farm located in the Romagna region (Italy) during the second week of September 2023 at commercial harvest.

FRED® (Origine group) variety began in early 2000 at the Agroscope

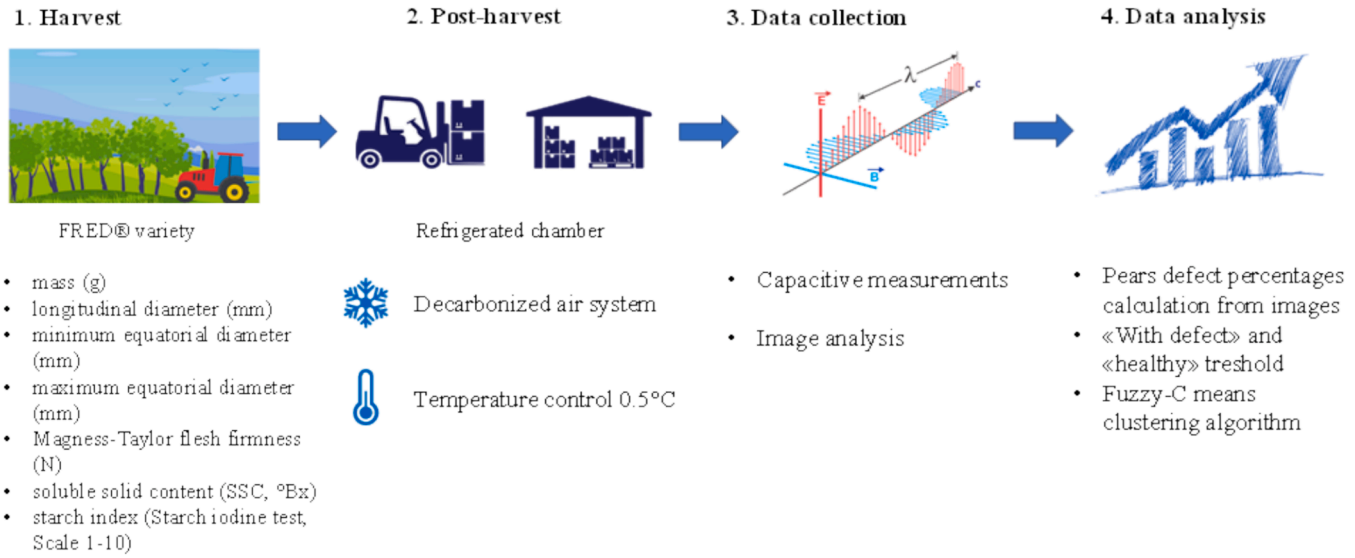

Fig. 1. Experimental plan design.

research station in Conthey, Switzerland, to obtain resistant genetic material to fire blight. The genetic cross between the Canadian variety "Harrow Sweet", tasty and tolerant to the aforementioned disease, and a Dutch variety called "Verdi", with high conservation potential and attractive red color, produced some selections, among which the one called CH201 is the most promising and selected for the present study. stood out and appeared to be among the most promising. From an agronomic point of view, the vegetative and productive habitus of Fred® does not seem to be characterized by a particular vigor, but with high productivity. Some uncertainty about the need to introduce pollinators arises from the fact that there is evidence of full production in monovarietal conditions. From the perspective of specialized plantings, the option that includes the introduction of pollinating varieties seems preferable. The solidity of the production also finds a valid ally in the high specific weight of the fruits, significantly higher than that of other varieties. Generally, fruits of this kind of variety with a diameter of less than 70 mm can easily reach a weight of 200 g. The harvest window of FRED® is currently included in the second ten days of September with a hardness that still appears to be sustained around a value of 7 kg/cm^2. The blushing facet of the fruits, and the yellow pulp perceptible at harvest, becomes intense, sometimes ochre, making them particularly attractive.

At harvest, the following values of dimensional characteristics and quality indices were measured on the first sample of fruits: mass (g), longitudinal diameter (mm), minimum equatorial diameter (mm), maximum equatorial diameter (mm), Magness-Taylor flesh firmness (N), soluble solid content (SSC, °Bx), and starch index (Starch iodine test, Scale 1–10). In detail, Magness-Taylor flesh firmness (N) and soluble solid content (°Bx) values were obtained by using a digital penetrometer (FTA-Fruit Texture Analyzer, 8 mm probe) and a digital refractometer (PR-1, ATAGO Co. Ltd., Tokyo, Japan), respectively.

After harvest, the second sample was stored in decarbonized atmosphere conditions, with 0.1 % CO_2 obtained with a decarbonization air system (Delta Gem ® Fruit Control) (Temperature = 0.5 °C) until the middle of January 2024. Capacitive measurements were conducted after the considered postharvest storage. Immediately before the electric acquisitions, fruit dimensional parameters in terms of mass (g), longitudinal diameter (mm), minimum equatorial diameter (mm), and maximum equatorial diameter (mm) were evaluated. After spectral assessments, Magness-Taylor flesh firmness (N) and soluble solid content (°Bx) were measured, and the fruit's internal browning was quantified through image analysis.

2.3. Capacitive measurements

2.3.1. Principle of detection

The material response under an applied electromagnetic field is described by the dielectric permittivity. The dielectric permittivity is composed of the real and imaginary parts, also known as the dielectric constant and loss factor. When an external electromagnetic field is applied to a material, the dielectric behaves as energy storage, while the loss factor is a measure of energy dissipation. The system developed focused on the evaluation of the capacitance, an electrical parameter. Capacitance is a function of the material dielectric constant, the material size, and the electrode distance. Accordingly, capacitance (Eq. (1) can be calculated as:

$$C = \varepsilon_r \varepsilon_0 \frac{A}{t} \quad (1)$$

C is the capacitance (F), ε_r is the relative dielectric constant of the material, ε_0 is the dielectric constant of free space (8.85×10^{-12}F/m), A is the area of capacitor plates (m^2) and t is the distance between parallel plates (m).

In this way, the internal defect of the fruit can be assessed by measuring the difference in capacitance as a result of different dielectric, as a function of frequency. When a pear is placed between the plates, the capacitance increases with an a-dimensional factor, the relative dielectric constant of the material interposed. Since capacitance is a function of electrode spacing, the plate distance was measured for each fruit and used as a correction coefficient, by dividing the capacitance with the distance value.

2.3.2. Instrumental chain and acquisition procedure

Electrical assessments were carried out by a self-assembled instrumental chain shown in Fig. 2.

The equipment consists of a parallel plate capacitor as a probe coupled with an LCR meter (LCR-8101G, GW-Instek, Good Will Instrument Co. Ltd, Taiwan), and interfaced with a PC. The capacitor is composed of two identical conducting stainless steel plates covered with a plastic film to isolate the proximal conductivity effects. The system has been calibrated with internal own procedures, for capacitance measurements. The parallel plates have to be put in contact with fruits with the mobile armature to adapt at different sample diameters. The contact of the pear with the plates can be considered point-like; moreover, it is an electrically insulated contact because the presence of a plastic film covering the conductive plates. For these reasons, no notable influence due to the contact of the pear with the electrodes is expected. On the contrary, measure of the plate distance was kept at each fruit to correct the capacitance measurements accordingly (mean distance and standard deviation: 65.2 ± 4.0 mm).

The probe has the following dimensions: 55.6 ± 0.1 mm (length), 1.3 ± 0.0 mm (width), 36.0 ± 0.1 mm (height), and a maximum plate distance of 83.0 mm. The capacitor was mounted on a plastic support to avoid movements of the cable connected to the LCR meter and avoid signal noise.

Measurements of capacitance were conducted at 5 ± 1°C and carried out in triplicate in the radio-frequency range from 100 Hz to 10 kHz (50 points, with a constant step of 202.041 Hz). The voltage was set to 1 V, and each measurement was automatically averaged 3 times.

2.3.3. Image analysis of internal browning

Immediately after capacitive acquisitions, pears were evaluated in terms of internal browning presence by using image analysis carried out using an electronic eye (visual analyzer VA400 IRIS Alpha M.O.S., France). The instrument is composed of a resealable chamber (420 × 560 mm^2), and a controlled with standardized light conditions: 98 CRI (color rendering index), D65 (light of a cloudy day at noon), 6700 °K (color temperature). The CCD camera (16 million colors) is positioned in the upper part of the chamber to allow high-resolution images with a built-in zoom calibrated and monitored completely automatically. The software (E-Eye software Alpha-Soft, version 14.0) is capable of acquiring data, analyzing images (RGB scale), and statistically processing the results. Two fluorescent LED channels illuminate the upper, lower, and back parts (to prevent shadows) of the cabin sides. The instrument performed an automatic calibration with a certified color checker, and image analysis (RGB scale or CIE L*a*b*). The image analysis of pears was set up with upper illumination only and a resolution of 2588 × 1942 pixels. The subsequent image analysis was performed by using ImageJ software (ImageJ 1.53 t, National Institutes of Health, USA). The images were acquired by placing 4 pears, half-cut, on a removable support blue colored at a 20 cm distance from the camera. The blue support allows the positioning of the pear in the defined grid. The reference grid created with blue plastic material is necessary to obtain a reference of standard dimensions. Varying the size of the pears, as long as they are positioned within the individual boxes that make up the grid, will not affect the calculations of the percentage of defect areas. As a first step, the pixels of the whole pear and the pixels of the defect areas were manually selected and saved as text files. The pixels of each portion were calculated by Excel files with cell coordinates that automatically extract the four-pear position and return the number of pixels. The damaged observations were identified in terms of the pixels' ratio

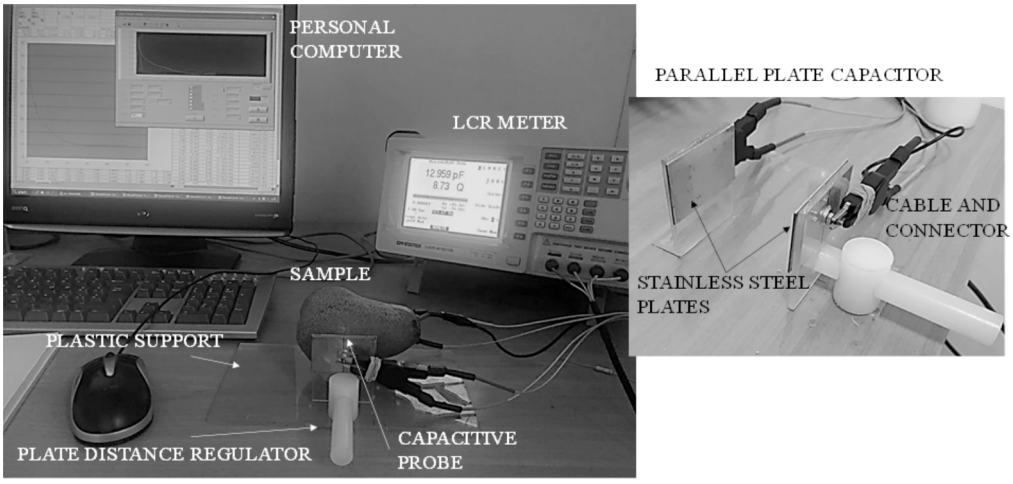

Fig. 2. Instrumental chain setup.

between the defected (browned) area and the total area. The calculated percentages were used to define a threshold score by visual appearance: that under or equal the 2 % pear does not show defects or only little browning is visible, while fruits with a score percentage higher than 2 revealed visible defects. According to image analysis (Fig. 3), pears with defect percentages lower than 2 %, show very slight or no change of pulp browning. In this way, the calculated percentages were used to define the two classes: "with defects" (> 2 % of pixels' ratio) and "healthy" (≤2% of pixels' ratio).

2.3.4. Statistical analysis

Capacitance acquisitions were arranged in a 59 (samples) × 50 (independent variables, capacitance values in the explored frequency range) X matrix. Data analysis was conducted by using JASP Team (2024) (Version 0.18.3, Computer software).

To classify pears according to the two identified classes, "with defects" (with internal defects, > 2 % of pixels' ratio) and "healthy" (without internal defects, (≤2% of pixels' ratio), the unsupervised Fuzzy-C means clustering algorithm was taken into consideration. As known and differently from K-means hard allocation, the Fuzzy-C means technique softly assigns observations to all clusters with varying degrees of membership [0,1]. The partitioning is conducted by following an iterative optimization of the objective function and, consequently, by updating the cluster membership and centers (prototypes) (Eq. (2) (Bezdek et al., 1984; Ferraro, 2024):

$$\min_{U,H} J_{FkM} = \sum_{i=1}^{n}\sum_{g=1}^{k} u_{ig}^{m} d^2(x_j, h_g)$$

$$u_{ig} \in [0,1] i = 1,\cdots,ng = 1,\cdots,k$$

$$\sum_{g=1}^{k} u_{ig} = 1 i = 1,\cdots,n \quad (2)$$

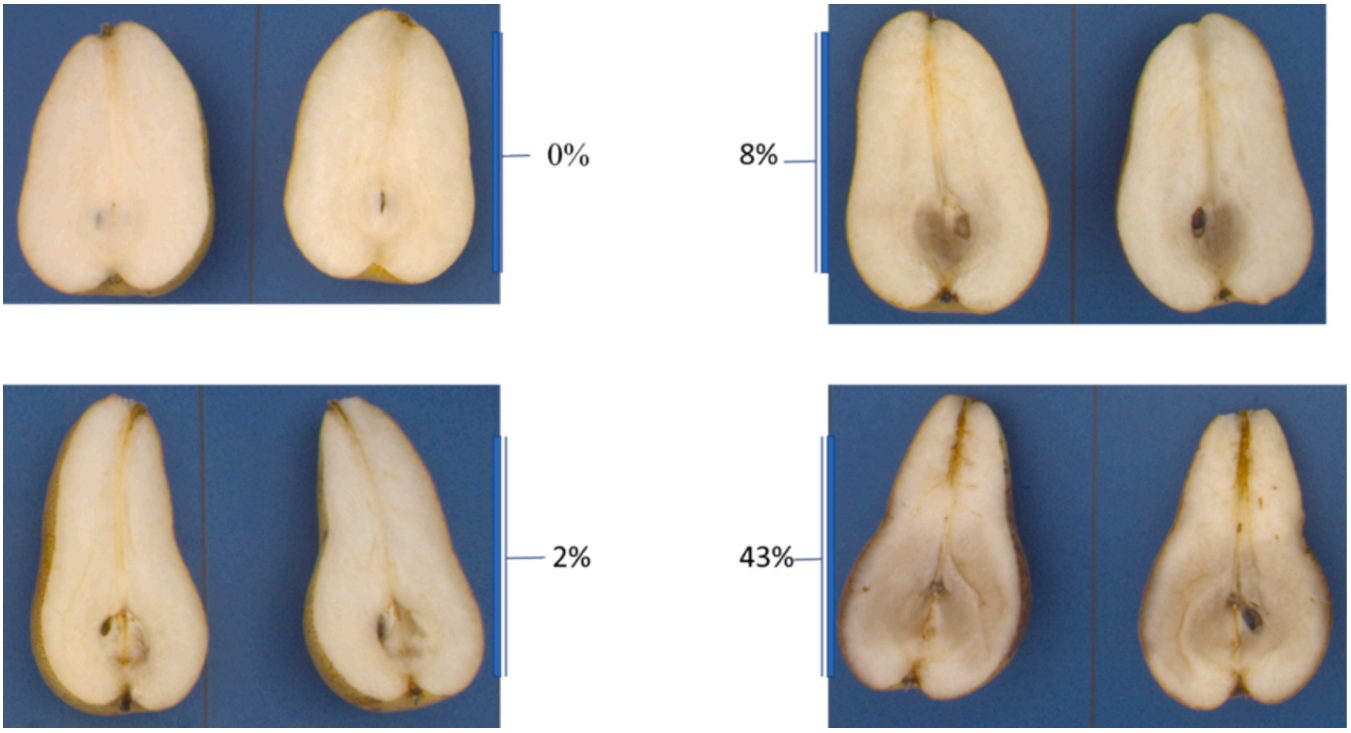

Fig. 3. Image analysis and damage scores pixels' ratio between the defected area and the total area.

where: $(k \times p)H$ is the prototype matrix with each row the prototype of cluster g; $(n \times k)U$ is the membership degree matrix shows the degree of observation i to cluster g; $d^2(x_j, h_g)$ is the square Euclidean distance between observation i and prototype g. Initial clustering prototypes were randomly determined and a maximum number of iterations (25) and a fuzziness parameter (2) were set up for the fixed number of clusters (2). The main results were expressed in terms of the percentage of correct classification samples and model performance (maximum and minimum diameter in Euclidean distance, Pearson's γ, and model-explained variance). A two-dimensional t-SNE clustering plot (random starting values) was used to show the relative distances between observations and clusters. The t-SNE algorithm aims at embedding high-dimensional points by respecting similarities between them (Van Der Maaten and Hinton, 2008).

3. Results and discussion

3.1. Destructive assessments

Table 1 shows a descriptive summary of the characteristics of the two samples of 59 pears each (at harvest and after the postharvest storage) in terms of mean values and standard deviations of the dimensional and qualitative parameters.

In addition, at harvest, pear samples were also characterized by a mean value of the starch index of 5.3 (±1.7).

As described above, percentages of internal defects were calculated, according to the material and method section, starting with image analysis. Fig. 3 shows examples of acquired pear images according to the percentages of pixels' ratio between the defective area and the total area.

Since characterized by percentage values of the of pixels' ratio (between the defected area and the total area) lower than 2 %, 42 % of the considered fruits were identified as "healthy". The remaining 58 % of pears showed the following distribution of the percentage values of the of pixels' ratio: mean, 7.1 %; standard deviation, ± 7.1 %; minimum, 2.4 %; maximum, 42.5 %. All fruits were not affected by the presence of internal cavities.

3.1.1. Capacitive measurements

It is known that rapid and non-destructive methods for food quality assessment were usually performed by using dielectric properties (Ryynänen, 1995). Concerning the internal quality of fruit, the radiofrequency range was previously explored by using Magnetic Induction Spectroscopy (MIS) on avocados to estimate ripeness (O'Toole et al., 2023). Accordingly, the capacitance was exploited for contactless fruit internal quality classification, as the penetration depth, in the very low frequency region explored, is suitable for whole fruit investigation. Capacitance in the presence of pear fruit ranges from about 10 to 18 pF. Averaged capacitive signals of pear fruits at 5 °C, after normalization on the parallel plate distance of each fruit, were shown in Fig. 4.

The capacitance spectra are the response of the applied field to the dielectric interposed, the pear, as a function of different chemical-physical compositions. The capacitance system is not a direct measurement of the internal defect, but a fingerprint of the fruit analyzed. Thus, the differences in spectral data can be related to fruit disease, which as an example can be verified for water distribution or different carbohydrate constituents' concentrations. Particularly considering foodstuffs with high moisture, water is the principle responsible for

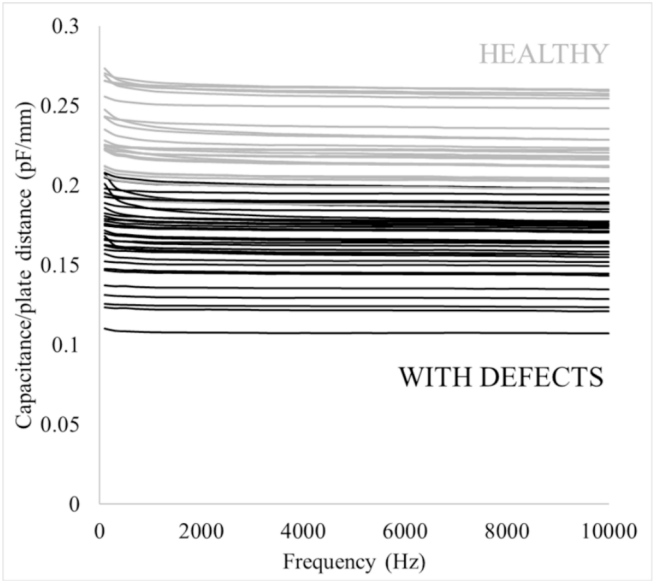

Fig. 4. The capacitance spectra (divided by plate distance) of pear fruit in the radiofrequency range are classified according to two classes: "healthy" and "with defects".

dielectric properties modification (Nelson and Trabelsi, 2008). In detail, the water content induces an increase of the dielectric constant, as a function of the polarization effect, otherwise water electric charges are easily polarized under an electric field. The increase in water polarized charges produces a greater electric filed induction, and thus a capacitance raises (Venkatesh and Raghavan, 2005).

3.1.2. Clustering

Table 2 shows the main results of the Fuzzy-C means clustering algorithm used to classify pears according to the two clusters, "with defects" and "healthy".

As evidenced, the Fuzzy-C means clustering algorithm was rather able to correctly classify pears according to the presence of internal defects (91 % of correct classifications). The three fruits incorrectly classified as "healthy" showed percentage values of pixels' ratio (between the defected area and the total area) from 2.8 % to 3.7 %. The Silhouette score, a measure of clustering quality (in terms of a measure of compactness and separation), evidences a misclustering when close to "-1", a weak structure when close to "0", and a strong clustering when close to "+1" (Rawashdeh and Ralescu, 2012). The appreciable clustering results can be also expressed, based on Euclidean distance, in terms of maximum diameter (16.5), minimum separation (0.778), and Pearson's γ (0.606). This last index represents the correlation and "0–1" vector (0 = same cluster; 1 = different clusters) (Zhang et al., 2009).

The two-dimensional t-SNE clustering plot, used to show the relative distances between observations and clusters, is shown in Fig. 5.

As can be appreciated, similarities and dissimilarities between observations according to the value of the pixels' ratio can be easily visualized in the two-dimensional clustering plot.

The proposed technique based on the capacitance can be exploited to classify pears according to internal defects, but it should be considered that tests were carried out at one ripening stage. During storage, the dielectric properties of the pear can change due to chemical and physical

Table 1
Mean values and standard deviations of the two independent batches of pear characteristics at harvest and after the CA postharvest storage.

Sample	Mass		Long. diam.		Min. eq. diam.		Max.eq. diam.		Magness-Taylor flesh firmness		Soluble solid content	
Harvest	242	±31 g	102	±10 mm	68	±4 mm	69	±4 mm	68.9	±6.8 N	15.7	±1.4 °Bx
Postharvest storage	258	±34 g	102	±10 mm	70	±4 mm	71	±4 mm	51.2	±5.4 N	18.0	±1.3 °Bx

Table 2
Fuzzy-C means clustering analysis results in terms of % of classification of two clusters: "with defects" and "healthy".

Cluster	Number of pears (total = 59)	Correct classification per cluster (%)	Explained proportion within-cluster heterogeneity	Within the sum of squares	Silhouette score
"With defects" (> 2 % of pixels' ratio)	34	91	0.601	556.2	0.576
"Healthy" (≤ 2 % of pixels' ratio)	25	88	0.399	368.5	0.575

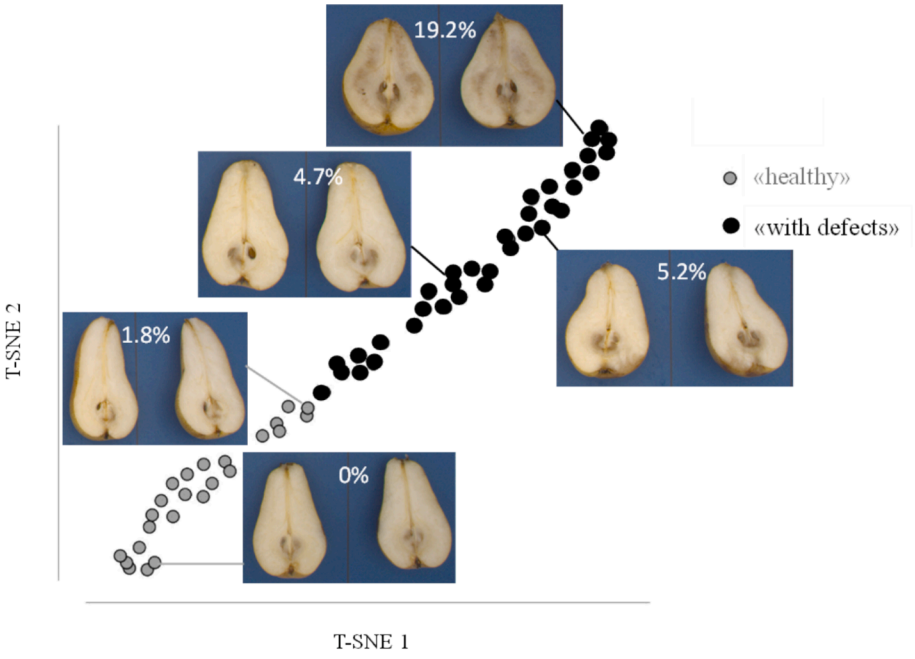

Fig. 5. t-SNE clustering plot.

modification also consider the ripening stage (García et al., 2004; Guo et al., 2011; Seo and Song, 2023; Soltani et al., 2011b). This can be a limitation of this study, even if the reliability could be implemented with additional samples at different ripening, to develop several models taking into consideration this important parameter. Another possible limitation could regard the possible presence of different kinds of internal defects. For example, internal cavities can occur in this variety and produce a dielectric behavior that the developed model does not take into account. The influence on the capacitance signal due to several ripening stages and the presence of internal cavities should considered in future works.

4. Conclusion

A parallel plate capacitor instrumental chain was exploited to predict internal browning in a new variety of pear fruit. The possibility of classifying the observations into two classes, "whit defect" and "healthy" fruit was explored with fuzzy C-means clustering analysis starting from capacitance spectral information. A global ("with defects" and "healthy") classification capacity of 89.5 % of samples was observed. The system proposed is rapid, cheap, and contactless allowing non-destructive measurements with possible future development of online and at-line applications in the postharvest facilities. Furthermore, it is promising to detect internal browning defects occurring during post-harvest storage of pears. Future perspectives should regard the increase of the sample number and the exploration of a wide range of ripening stages to increase the robustness of the classification herein performed and the knowledge about the influence on the dielectric properties of other different internal damages.

CRediT authorship contribution statement

Eleonora Iaccheri: Writing – original draft, Methodology, Investigation, Formal analysis, Data curation, Conceptualization. **Annachiara Berardinelli:** Writing – original draft, Formal analysis, Data curation, Conceptualization. **Gianni Ceredi:** Writing – review & editing, Conceptualization. **Luigi Ragni:** Writing – review & editing, Formal analysis, Data curation, Conceptualization.

Declaration of competing interest

The authors declare that they have no known competing financial interests or personal relationships that could have appeared to influence the work reported in this paper.

Data availability

Data will be made available on request.

References

Berardinelli, A., Iaccheri, E., Franceschelli, L., Tartagni, M., Ragni, L., 2021. Non-destructive assessment of kiwifruit flesh firmness by a contactless waveguide device and multivariate regression analyses. IEEE J Emerg Sel Top Circuits Syst 11, 515–522. https://doi.org/10.1109/JETCAS.2021.3097095.

Bezdek, J.C., Ehrlich, R., Full, W., 1984. FCM: the fuzzy c-means clustering algorithm. Comput. Geosci. 10, 191–203. https://doi.org/10.1016/0098-3004(84)90020-7.

Cao, M., Zeng, S., Wang, J., Guo, W., 2023. Dielectric properties of peaches with and without skin during storage and their relationship to internal quality. Postharvest Biol. Technol. 204. https://doi.org/10.1016/j.postharvbio.2023.112433.

Carmignato S., Dewulf W., Leach R., 2017. Industrial X-ray computed tomography, Industrial X-Ray Computed Tomography. Springer International Publishing. doi: 10.1007/978-3-319-59573-3.

Clark', C.J., Hockings, P.D., Joyce', D.C., Mazucco, R.A., 1997. Application of magnetic resonance imaging to pre-and post-harvest studies of fruits and vegetables. Postharvest Biol. Technol. 11, 1–21. https://doi.org/10.1016/S0925-5214(97)01413-0.

Colnago, L.A., Andrade, F.D., Souza, AC.A., Azeredo, R.B.V., Lima, A.A., Cerioni, L.M., Osán, T.M., Pusiol, D.J., 2014. Why is inline NMR rarely used as industrial sensor? Challenges and opportunities. Chem. Eng. Technol. 37, 191–203. https://doi.org/10.1002/ceat.201300380.

Evans K. (Kate), 2020. Achieving sustainable cultivation of apples. should be replaed with: Watkins, C. (Ed.). (2020). Advances in postharvest management of horticultural produce (1st ed.). Burleigh Dodds Science Publishing. https://doi.org/10.1201/9781003047650.

Ferraro, M.B., 2024. Fuzzy k-means: history and applications. Econom Stat 30, 110–123. https://doi.org/10.1016/j.ecosta.2021.11.008.

Franck, C., Lammertyn, J., Ho, Q.T., Verboven, P., Verlinden, B., Nicolaï, B.M., 2007. Browning disorders in pear fruit. Postharvest Biol. Technol. https://doi.org/10.1016/j.postharvbio.2006.08.008.

García, A., Torres, J.L., De Blas, M., De Francisco, A., Illanes, R., 2004. Dielectric characteristics of grape juice and wine. Biosyst. Eng. 88, 343–349. https://doi.org/10.1016/j.biosystemseng.2004.04.008.

Guo, W., Zhu, X., Nelson, S.O., Yue, R., Liu, H., Liu, Y., 2011. Maturity effects on dielectric properties of apples from 10 to 4500 MHz. LWT 44, 224–230. https://doi.org/10.1016/j.lwt.2010.05.032.

Guo, W., Fang, L., Liu, D., Wang, Z., 2015. Determination of soluble solids content and firmness of pears during ripening by using dielectric spectroscopy. Comput. Electron. Agric. 117, 226–233. https://doi.org/10.1016/j.compag.2015.08.012.

Han, D., Tu, R., Lu, C., Liu, X., Wen, Z., 2006. Nondestructive detection of brown core in the Chinese pear "Yali" by transmission visible-NIR spectroscopy. Food Control 17, 604–608. https://doi.org/10.1016/j.foodcont.2005.03.006.

Hernández-Sánchez, N., Hills, B.P., Barreiro, P., Marigheto, N., 2007. An NMR study on internal browning in pears. Postharvest Biol. Technol. 44, 260–270. https://doi.org/10.1016/j.postharvbio.2007.01.002.

Khaled, D.E., Novas, N., Gazquez, J.A., Garcia, R.M., Manzano-Agugliaro, F., 2015. Fruit and vegetable quality assessment via dielectric sensing. Sensors (Switzerland). https://doi.org/10.3390/s150715363.

Lammertyn, J., Dresselaers, T., Van Hecke, P., Jancsók, P., Wevers, M., Nicolaï, B.M., 2003. MRI and X-ray CT study of spatial distribution of core breakdown in "Conference" pears. Magn. Reson. Imaging 21, 805–815. https://doi.org/10.1016/S0730-725X(03)00105-X.

Lwin, H.P., Torres, C.A., Rudell, D.R., Lee, J., 2023. Chilling-related browning of 'Wonhwang' pear cortex is associated with the alteration of minerals and metabolism. Sci. Hortic. 321. https://doi.org/10.1016/j.scienta.2023.112321.

Mei, M., Li, J., 2023. An overview on optical non-destructive detection of bruises in fruit: technology, method, application, challenge and trend. Comput. Electron. Agric. https://doi.org/10.1016/j.compag.2023.108195.

Nelson, S.O., Trabelsi, S., 2008. Dielectric spectroscopy measurements on fruit, meat, and grain. Trans. ASABE 51, 1829–1834.

Nugraha, B., Verboven, P., Janssen, S., Wang, Z., Nicolaï, B.M., 2019. Non-destructive porosity mapping of fruit and vegetables using X-ray CT. Postharvest Biol. Technol. 150, 80–88. https://doi.org/10.1016/j.postharvbio.2018.12.016.

O'Toole, M.D., Glowacz, M., Peyton, A.J., 2023. Bioimpedance measurement of avocado fruit using magnetic induction spectroscopy. IEEE Transactions on AgriFood Electronics 1, 99–107. https://doi.org/10.1109/tafe.2023.3303177.

Ragni, L., Berardinelli, A., Cevoli, C., Valli, E., 2012. Assessment of the water content in extra virgin olive oils by Time Domain Reflectometry (TDR) and Partial Least Squares (PLS) regression methods. J. Food Eng. 111, 66–72. https://doi.org/10.1016/j.jfoodeng.2012.01.028.

Rawashdeh M., Ralescu A., 2012. Fuzzy Cluster Validity with Generalized Silhouettes.

Ryynänen, S., 1995. The electromagnetic properties of food materials: a review of the basic principles. J. Food Eng. 26, 409–429. https://doi.org/10.1016/0260-8774(94)00063-F.

Seo, H.J., Song, J., 2023. Detection of internal browning disorder in 'Greensis' pears using a portable non-destructive instrument. Horticulturae 9. https://doi.org/10.3390/horticulturae9080944.

Sipahioglu, O., Barringer, S.A., 2003. Dielectric properties of vegetables and fruits as a function of temperature, ash, and moisture content. J. Food Sci. 68, 234–239. https://doi.org/10.1111/j.1365-2621.2003.tb14145.x.

Soltani, M., Alimardani, R., Omid, M., 2011a. Evaluating banana ripening status from measuring dielectric properties. J. Food Eng. 105, 625–631. https://doi.org/10.1016/j.jfoodeng.2011.03.032.

Streif J., Xuan H., Saquet A.A., Rabus C., 2001. CA-storage Related Disorders in "Conference" Pears. Proc. 4th. Int. Conf. On Postharvest, Eds. R. Ben-Arie S. Philosoph-Hadas, Acta Hort. 553, ISHS 2001. DOI: 10.17660/ActaHortic.2001.553.153.

Teixeira A.R.N., Ferreira R.M.B., 2003. Teixeira Ferreira 2003, in: Elsevier (Ed.), Encyclopedia of Food Science and Nutrition. doi: 10.1016/B978-0-12-375083-9.00011-8.

Tempelaere, A., Van De Looverbosch, T., Kelchtermans, K., Verboven, P., Tuytelaars, T., Nicolai, B., 2023. Synthetic data for X-ray CT of healthy and disordered pear fruit using deep learning. Postharvest Biol. Technol. 200. https://doi.org/10.1016/j.postharvbio.2023.112342.

Van De Looverbosch, T., Rahman Bhuiyan, M.H., Verboven, P., Dierick, M., Van Loo, D., De Beenbouwer, J., Sijbers, J., Nicolaï, B., 2020. Nondestructive internal quality inspection of pear fruit by X-ray CT using machine learning. Food Control 113. https://doi.org/10.1016/j.foodcont.2020.107170.

Van De Looverbosch, T., He, J., Tempelaere, A., Kelchtermans, K., Verboven, P., Tuytelaars, T., Sijbers, J., Nicolai, B., 2022. Inline nondestructive internal disorder detection in pear fruit using explainable deep anomaly detection on X-ray images. Comput. Electron. Agric. 197. https://doi.org/10.1016/j.compag.2022.106962.

Van Der Maaten, L., Hinton, G., 2008. Visualizing data using t-SNE. J. Mach. Learn. Res. 9, 2579–2605.

Venkatesh M.S., Raghavan G.S. V, 2005. An overview of dielectric properties measuring techniques, CANADIAN BIOSYSTEMS ENGINEERING.

Zerbini, P.E., Grassi, M., Cubeddu, R., Pifferi, A., Torricelli, A., 2002. Nondestructive detection of brown heart in pears by time-resolved reflectance spectroscopy. Postharvest Biol. Technol. 25, 87–97. https://doi.org/10.1016/S0925-5214(01)00150-8.

Zhang M., Zhang W., Sicotte H., Yang P., 2009. A new validity measure for a correlation-based fuzzy C-means clustering algorithm, in: Proceedings of the 31st Annual International Conference of the IEEE Engineering in Medicine and Biology Society: Engineering the Future of Biomedicine, EMBC 2009. IEEE Computer Society, pp. 3865–3868. doi: 10.1109/IEMBS.2009.5332582.

Zhang, Q., Huang, W., Wang, Q., Wu, J., Li, J., 2022. Detection of pears with moldy core using online full-transmittance spectroscopy combined with supervised classifier comparison and variable optimization. Comput. Electron. Agric. 200. https://doi.org/10.1016/j.compag.2022.107231.

Zhang, H., Wang, K., Gu, J., Feng, Z., Zhang, F., 2024. Application of statistical features in vibro-acoustic signals to detect early browning disorder in pears compared with food chemistry method. J. Electr. Syst. 20 (2), 190–199. https://doi.org/10.52783/jes.1125.

Zhao, K., Zha, Z., Li, H., Wu, J., 2021. Early detection of moldy apple core based on time-frequency images of vibro-acoustic signals. Postharvest Biol. Technol. 179. https://doi.org/10.1016/j.postharvbio.2021.111589.